



Chemical composition and size distributions of coastal aerosols observed on the US East Coast

Lili Xia, Yuan Gao*

Department of Earth and Environmental Sciences, Rutgers University, Newark, NJ 07102, United States

ARTICLE INFO

Article history:

Received 10 July 2009

Received in revised form 20 December 2009

Accepted 5 January 2010

Available online 20 January 2010

Keywords:

Coastal aerosol

Size distributions

Chemical compositions

Fe solubility

ABSTRACT

Characterization of coastal aerosols is important to the study of the atmospheric input of nutrients to the adjacent marine and the ocean ecosystems. Over a land–ocean transition zone, however, aerosol composition could be strongly modified by anthropogenic emissions and transport processes. This work focuses on examining aerosol properties, in particular chemical composition, particle-size distributions and iron (Fe) solubility, over the US East Coast, an important boundary for the transport of continental substances from North America to the North Atlantic Ocean. Fourteen sets of bulk aerosol samples and three sets of size-segregated aerosol samples were collected in southern New Jersey on the US East Coast during 2007 and 2008. Samples were analyzed by IC, ICP-MS and UV spectroscopy. The major chemical components were nitrate, non-sea-salt sulfate (NSS-sulfate), ammonium and chloride, accounting for ~70% of the total mass. A typical bimodal mass-size distribution was observed, with the major peak from 0.36 μm to 0.56 μm and the minor one from 3.6 μm to 5.6 μm in diameters. Different individual components showed different mass-size distributions. Pollution-derived substances, such as vanadium and NSS-sulfate of non-biogenic origin, were mostly in the fine mode, while crustal elements, such as aluminum and iron, were mainly in the coarse mode. At this location, the concentrations of soluble ferrous species (Fe(II)s) in aerosols ranged from 50 to 518 pmol m^{-3} , accounting for ~17% of the total Fe (Fe_T) mass in bulk samples. The average Fe solubility observed at this location was 18%, higher than those over remote oceans. Fe solubility showed an inverse correlation with Fe_T concentrations, which could be the result of different particle sizes. In addition, high Fe solubility was associated with high molar ratios of NSS-sulfate to Fe_T and oxalate to Fe_T , indicating that inorganic and organic acidic components and anthropogenic emissions may highly affect Fe solubility in this region.

© 2010 Elsevier B.V. All rights reserved.

1. Introduction

Aerosols over the coastal regions are important for understanding the transport of atmospheric substances from the continents to the ocean, the major pathway of nutrient delivery to the remote ocean (Duce and Tindale, 1991; Fung et al., 2000). In addition, atmospheric deposition plays an important role in nutrient input to certain coastal regions (Hutchins and Bruland, 1998), and aerosol measurements at coastal sites can assist in estimating atmospheric fluxes of nutrients to a particular coastal ecosystem, supporting mass balance studies (Yaaqub et al., 1991; Chester et al., 1993; Kane et al., 1994). On the other hand, the composition of aerosols over the coastal regions is complicated, as aerosols of continental origin could be modified significantly before they are transported to the remote ocean by both anthropogenic and natural processes, such as interactions with air pollutants and intensive meteorological events (Whelpdale and Moody, 1990). For example, atmospheric pollutants from anthropo-

genic emissions, such as organic acids, may affect aerosol size distributions (de Gouw et al., 2005; Brock et al., 2008) and properties of certain trace elements, such as Fe solubility, and consequently influence trace metal bioavailability (Spokes et al., 1994).

The US East Coast is an important boundary between North America and the North Atlantic Ocean. Aerosols from different sources transported over this region could be modified significantly before reaching the remote Atlantic. There have been a number of studies of aerosol characteristics on the US East Coast, including the total aerosol mass (Novakov et al., 1997; Castanho et al., 2005), trace metal concentrations (Church et al., 1990; Malm and Sisler, 2000; Pike and Moran, 2001), water-soluble ion concentrations (Tolocka et al., 2001; Song et al., 2001; Zhao and Gao, 2008) and mass-size distributions (Brock et al., 2008; Zhao and Gao, 2008). High anthropogenic signatures associated with aerosols were found in this region (Malm and Sisler, 2000), such as high concentrations of nickel, vanadium, lead and zinc from oil combustion, nitrate from motor vehicles (Song et al., 2001), and sulfate and ammonium from industrial and power generation facilities (Brock et al., 2008). As the atmosphere is the major pathway for the input of certain elements to the ocean, such as iron (Duce et al., 1991) and anti-

* Corresponding author. Tel.: +1 973 353 1139; fax: +1 973 353 1965.

E-mail address: yuangaoh@andromeda.rutgers.edu (Y. Gao).

consequently affect coastal marine ecosystems, as well as exert potential effects on oceanic ecosystems (Jickells, 1998; Doney et al., 2007).

Iron is an important element relevant to marine biogeochemical cycles, as it is a limiting nutrient in phytoplankton growth (Martin, 1990; Duce et al., 1991; Falkowski et al., 1998; Morel and Price, 2003). The bio-uptake of Fe may depend on Fe solubility and speciation, in particular the dissolved forms of ferrous Fe, known as Fe(II)s, as Fe(II)s is believed to be more readily used by phytoplankton (Sunda, 2001), although Fe(II) may not always be bioavailable (Visser et al., 2003) and Fe(III) could be used by marine organisms as well (Barbeau et al., 2001). Aerosol Fe properties over coastal regions adjacent to large urban and industrial centers could be strongly affected by human activities, such as intensive combustion (Hoffmann et al., 1996) and interactions with anthropogenic pollutants (Chen and Siefert, 2004; Sedwick et al., 2007; Buck et al., 2008a). In addition, complex meteorology conditions favoring photochemical reactions and cloud cycling over the coastal regions may also modify Fe properties (Zhu et al., 1992; Jickells and Spokes, 2001; Desboeufs et al., 2001). Therefore, Fe properties over coastal regions deserve more attention. With increased concerns about anthropogenic emissions and their effects on Fe solubility and deposition over both the remote oceans and coastal regions (Luo et al., 2008), the study of Fe properties in polluted coastal marine atmospheres is critically needed.

To characterize aerosol properties including Fe solubility and speciation on the US East Coast, sampling of both bulk and size-segregated aerosol particles was carried out during spring 2007 and summer 2008 at a coastal site in southern New Jersey. In this paper, we discuss the chemical composition of aerosols along with their possible sources and present mass-size distributions of aerosols from different sources. We also discuss factors controlling Fe solubility. Results from this work will be valuable for quantifying coastal aerosol properties and filling the data gap for this region. The *in situ* data generated from this work will also be useful for modeling Fe deposition fluxes to both the coastal and the open oceans.

2. Methodology

2.1. Aerosol sampling

The sampling site was located at Tuckerton (39°36'N, 74°20'W), housed at the Rutgers University Marine Field Station in southern New Jersey on the US East Coast (Fig. 1). Two series of samples were taken in spring 2007 and summer 2008. During March 2007, fourteen diel samples were collected on Whatman-41 filters (Whatman International Ltd., England) by a High-Volume sampler, Model 500EL (Aquaero Tech, Miami, FL). In June 2008, three sets of size-segregated samples were taken using a non-rotating 10-stage Micro-Orifice Uniform Deposit Impactor (MOUDI) (MSP Corporation, Shoreview, MN) (Table 1), with a Teflon filter (Pall Corporation, 1.0 μm pore size) as the sampling medium. The 50% cut-off mass median aerodynamic diameters (MMAD) of MOUDI are 0.056, 0.10, 0.18, 0.32, 0.56, 1.0, 1.8, 3.2, 5.6, 10 and 18 μm. Our tests on non-rotating MOUDI samples collected at another site in New Jersey indicate that the relative differences in trace metal concentrations from duplicate MOUDI samples varied from 5.1% to 17%, with an average value of 11%. We note that numbers of samples collected are limited, due to financial restrictions; we hope more sampling work could be done in the near future to allow us to expand the effort at this location.

As shown in Table 1, there were differences in meteorology conditions between the two sampling periods. In March 2007, the ambient temperatures varied from −3.3 °C to 25 °C with an average of 8.3 °C; the relative humidity ranged from 24% to 93%. During this period, two rain events took place: light rain on March 11 and rain from March 15–17. In June 2008, the average ambient temperature was 21 °C, higher than that in March 2007, varying between 15 °C and 32 °C, and the averaged relative humidity was 85%. In addition, the surface-level winds in March 2007 were more from the ocean sector and stronger compared with those in June 2008 (Fig. 2); while results of air-mass back trajectories at altitude of 500 m, 1000 m and 2000 m

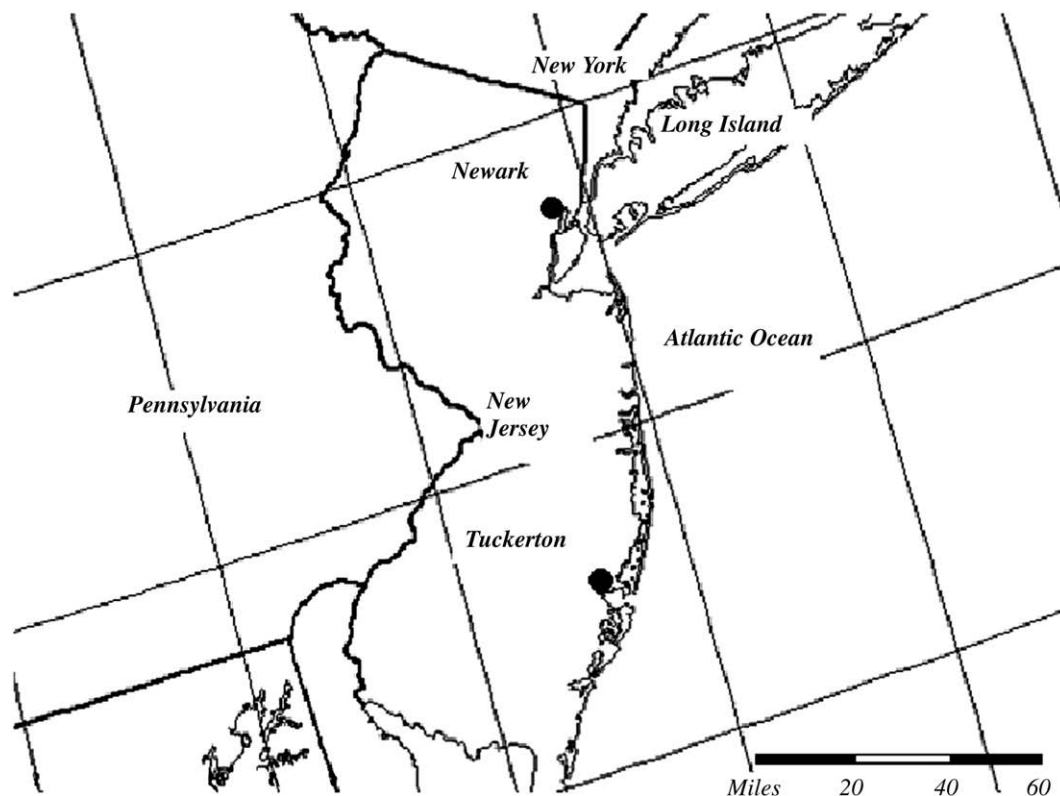


Fig. 1. Map of the sampling locations.

Table 1
Sampling information.

Sample type	Sample ID	Sampling ^a (starting date (h))	Temperature (°C)	Relative humidity (%)	Precipitation (mm h ⁻¹)
Bulk samples	1	03/09/07 (25)	5.1 (-3.3–14)	74 (53–93)	0
	2	03/10/07 (N14)	8.6 (6.1–10)	81 (68–90)	0.067
	3	03/11/07 (D10)	11 (6.1–14)	38 (28–59)	0
	4	03/11/07 (N11)	0.50 (-1.7–5.0)	64 (49–72)	0
	5	03/12/07 (D11)	8.6 (-2.2–12)	42 (24–75)	0
	6	03/12/07 (N13)	4.2 (2.2–6.1)	70 (53–82)	0
	7	03/13/07 (D10)	12 (5.6–16)	53 (39–73)	0
	8	03/13/07 (N14)	9.5 (8.3–12)	74 (64–77)	0
	9	03/14/07 (D9.4)	16 (11–18)	58 (50–74)	0
	10	03/14/07 (N14)	13 (12–15)	72 (62–80)	0
	11	03/15/07 (D10)	19 (13–25)	51 (39–67)	0
	12	03/15/07 (N14)	5.4 (3.3–11)	82 (63–89)	1.0
	13	03/16/07 (D8.4)	3.0 (2.8–3.3)	88 (86–89)	1.9
	14	03/16/07 (18)	0.30 (-2.2–3.3)	85 (70–92)	0.83
Size-segregated samples	I	05/30/08 (94)	19 (15–25)	81 (56–98)	1.4
	II	06/04/08 (119)	20 (15–32)	91 (61–100)	0.45
	III	06/09/08 (121)	23 (19–29)	82 (60–94)	0

^a N refers to nighttime sampling duration (mostly between 7 pm–8 am); D refers to daytime sampling duration (mostly between 8 am–7 pm).

indicated that the MOUDI samples in 2007 were affected more by air masses of inland origins (Fig. 3). The different conditions between the two sampling periods could contribute to the observed concentration differences between these two types of samples.

2.2. Chemical analysis

2.2.1. Water-soluble ions

The analysis of water-soluble ions in aerosol samples was carried out by an Ion Chromatography System (ICS-2000, Dionex) at the atmospheric chemistry laboratory at Rutgers University at Newark, following the procedures in Zhao and Gao (2008). Briefly, a portion of the Whatman-41 filter and Teflon filter were cut and put into an acid-cleaned test tube, and extracted with Milli-Q water (18 MΩ cm⁻¹) (Milli-Q Academic System, Millipore Corporation) in an ultrasonic bath for 30 min at room temperature. Then the leachate was filtered through a PTFE syringe filter (Fisher brand, 0.4 μm pore size) before being injected into the IC system. An AS11 analytical column (2×250 mm², Dionex), KOH eluent generator (EGC II KOH, Dionex) and 100 μl sample loop were employed for the determinations of selected anions (fluoride, acetate, propionate, formate, methanesulfonate, chloride, nitrate, succinate, malonate, sulfate and oxalate). Selected cations (sodium,

potassium, ammonium, magnesium and calcium) were determined by the same IC system with a CS12A analytical column (2×250 mm², Dionex), methanesulfonic acid (MSA) (EGC II MSA, Dionex) as the eluent and a 25 μl sample loop. The method detection limit for major anions, including sulfate, nitrate, chloride, oxalate, malonate, and succinate, is <9 μg l⁻¹. The recovery falls in the range of 78–101%, and the precision of the analytical procedures is ~1%.

2.2.2. Trace metals

The concentrations of aluminum (Al), antimony (Sb), cadmium (Ca), chromium (Cr), cobalt (Co), copper (Cu), iron, lead (Pb), manganese (Mn), nickel (Ni), scandium (Sc) vanadium (V) and zinc (Zn), were determined by Inductively Coupled Plasma Mass Spectrometry (ICP-MS, Finnigan™ ELEMENT2, Thermo Scientific) at the Institute of Marine and Coastal Science, Rutgers University. Portions of the Whatman-41 filter and Teflon filter were cut and digested with 0.857 ml concentrated HNO₃ (Optima A460-500, Fisher Scientific) and 12 μl concentrated HF (Optima A463-250, Fisher Scientific) in a Microwave Accelerated Reaction System (MARS, CEM Corporation). There were three steps in the digestion process: (1) heating to 170 ± 5 °C in 5.5 min, (2) remaining at 170 ± 5 °C for 30 min for the completion of digestion, and (3) cooling down for 20 min. Then, digested solutions were diluted

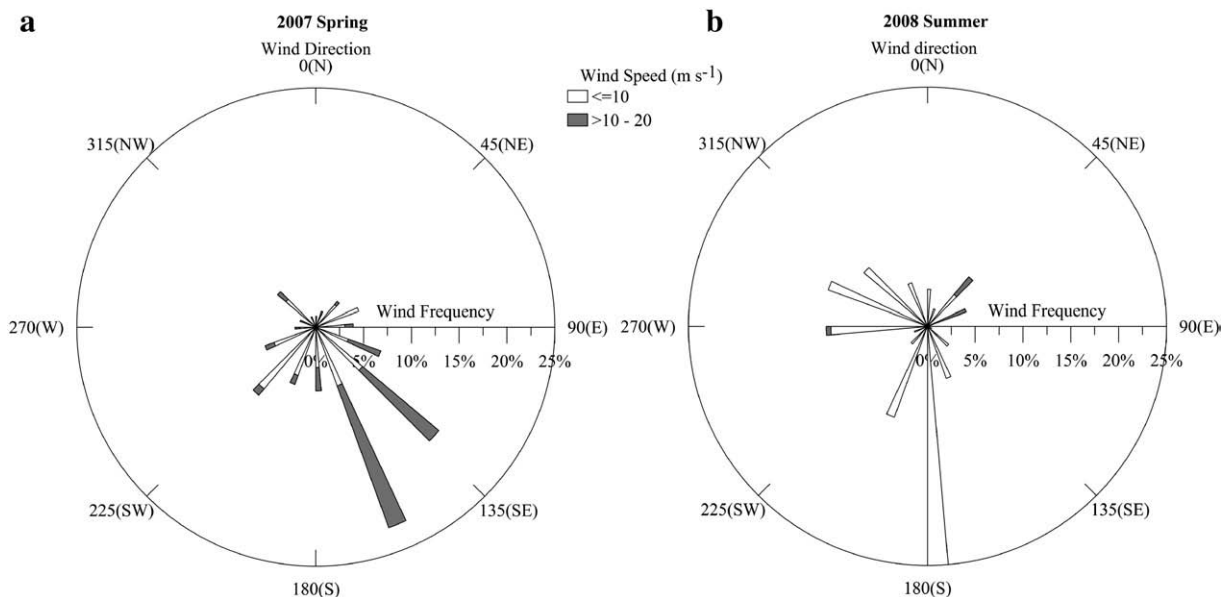


Fig. 2. Wind speed and direction: (a) bulk sampling during spring 2007; and (b) size-segregated sampling during summer 2008.

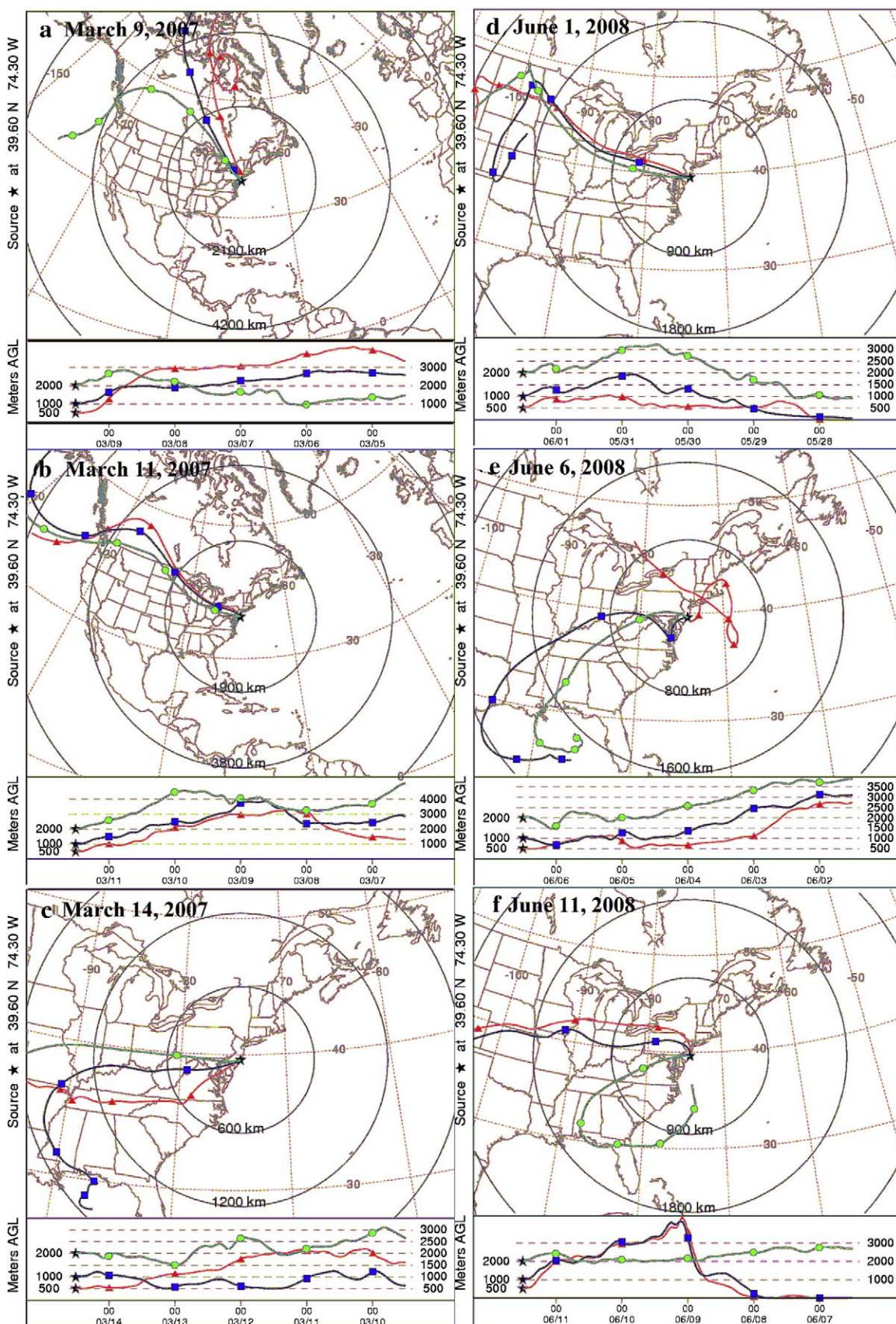


Fig. 3. Air-mass back trajectories (AMBTs) were calculated from the National Oceanic and Atmospheric Administration (NOAA) GDAS meteorology database using the Hybrid Single-Particle Lagrangian Integrated Trajectories (HY-SPLIT) program. AMBTs were performed at 500, 1000 and 2000 m height levels over the sampling location, and started at noon of each examined day with backward 5 days. Panels a, b, and c are for bulk samples: from March 9 to March 10, air masses were more from NNEW; from March 11 to March 13, air masses were more from NW; and starting from March 14, the SW air mass was dominant. Panels d, e, and f are for size-segregated samples.

with Milli-Q water to reach a solution acidity of ~4% before injection into the ICP-MS system. To quantify the digestion recovery, Reference Materials No. SRM 2783 (National Institute of Standard and Technology) were digested in the same way as the samples. The results showed that the recoveries of Al, Cu, Fe, Pb, V, Zn, Co, and Cr ranged from 91% to 103%. The detection limits for all trace metals were less than 1 ppt and the precision of the method was ~2%. The overall average blank levels were 4% for Whatman-41 filters and 2% for Teflon filters relative to samples. All numbers for samples were obtained after subtraction of their appropriate blank values.

2.2.3. Soluble ferrous (Fe(II)s)

The concentrations of Fe(II)s in aerosols were measured by absorption spectroscopy at 562 nm using a UV-1700 system (Shimadzu, Columbia, MD) at the atmospheric chemistry laboratory at Rutgers University at Newark, following methods by Stookey (1970), Zhu et al. (1997) and Xu and Gao (2008). The detailed procedure is shown in Fig. 4. Briefly, for size-segregated samples collected on Teflon filter: Half of the filter from each sample was cut and placed into a 50 ml acid-cleaned test tube and leached with 45 ml 1 M NaCl solution. After 4 h, an 8 ml 5 M buffer solution made of ammonium acetate and 1.2 ml 0.05 M ferrozine solution were added into a 20 ml filtered leaching solution. Then, the complex of Fe(II)s and ferrozine was measured. For bulk samples collected on Whatman-41 filter: an eighth of filter was cut and placed into the same leaching solution for 5 min, followed with the same procedures for Teflon filter samples. In this study, the leaching solution, NaCl (1 M), was acidified to pH = 1.0 by HCl (Optima A466-250, Fisher Scientific), because high relative humidity condition at this location as indicated in Table 1 could induce a high ionic strength and pH as low as 1.0 in the aerosol (Zhu et al., 1992). The detection limit of the method was ~30 nM using 10 cm length glass cells. The total dissolved Fe (Fe(II) + Fe(III)) was measured by the same method after reduction of the Fe(III) by adding a reducing reagent, hydroxylamine hydrochloride. Soluble Fe(III) was determined as the difference between the total soluble iron and Fe(II). As Fe(II)s accounted for more than 99% of the total soluble Fe, we operationally defined Fe solubility as the percentage of Fe(II)s over the total Fe (Fe_T).

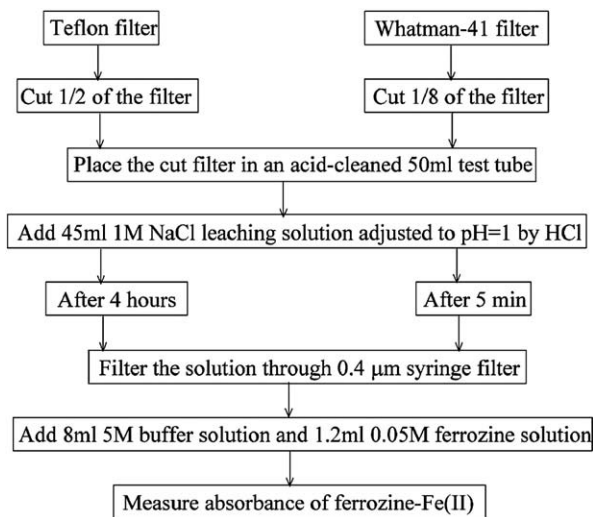


Fig. 4. Fe(II)s experimental procedure. Size-segregated samples collected on Teflon filter: Half filter was cut into a 50 ml acid clean test tube and leached by 45 ml 1 M NaCl solution (pH was adjusted to 1 by HCl). After 4 h, 8 ml 5 M buffer solution and 1.2 ml 0.05 M ferrozine solution were added into filtrated 20 ml extracted solution. Then, the complex of Fe(II)s and ferrozine was measured by the absorption at 560 nm. Bulk samples collected on Whatman-41 filter: An eighth of filter was cut and sunk into the same leaching solution for 5 min, and then followed all the same procedures to measure Fe(II)s.

3. Results and discussion

3.1. Chemical composition

Table 2 shows the average concentrations of chemical components in both bulk and size-segregated aerosol samples. In this study, the sum of 10 individual size concentrations from a MOUDI set was used as one segregated sample; chemical components include 13 trace metals, 11 anions and 5 cations. The concentrations of non-sea-salt (NSS) sulfate were calculated by subtracting sea-salt sulfate from the total sulfate using the typical sulfate-to-sodium mass ratio 0.25 in seawater (Millero and Sohn, 1992). We note that direct comparison between bulk and size-segregated samples may not be appropriate, as different collection periods and samplers may contribute to the variability of the observed concentrations between bulk and MOUDI samples (Buck et al., 2008b).

Trace metals accounted for ~1.0% of the total aerosol mass (sum of all chemical components measured), with Fe and Al being the major contributors. Aluminum is an indicator for mineral dust, comprising ~8.0% of crustal material in general (Taylor and McLennan, 1985). The total Al concentrations ranged from 107 to 10,490 pmol m⁻³ at this location, which was lower than those observed in some other coastal regions on the US East Coast, such as in New Castle, NH, and a coastal region in China (Gao et al., 1992; Pike and Moran, 2001) and was also lower than in the northwest Pacific Ocean and the north Atlantic Ocean where the dust influence was relatively strong (Arimoto et al., 1995; Buck et al., 2006, 2008a). At this location, several trace metals, such as Pb, V and Zn, were likely from anthropogenic emissions. Vanadium concentrations in bulk samples ranged from 9.0 to 146 pmol m⁻³, with an average of 69 pmol m⁻³, lower than other coastal regions where the average concentrations of V were from 118 pmol m⁻³ to 392 pmol m⁻³.

Table 2

The concentrations of chemical components in bulk and size-segregated samples.

Species	Unit	Bulk samples (2007 March)		Size-segregated samples (2008 June) ^a	
		N ^b	Mean (range)	N ^b	Mean (range)
Al	pmol m ⁻³	14	2694 (108–10,490)	3	3580 (2524–4527)
Cd	pmol m ⁻³	14	0.80 (0.25–1.7)	3	0.60 (0.54–0.69)
Co	pmol m ⁻³	14	1.4 (0.090–2.8)	3	2.4 (1.4–4.4)
Cr	pmol m ⁻³	13	7.6 (2.8–15)	3	64 (28–89)
Cu	pmol m ⁻³	13	29 (4.2–67)	3	48 (43–56)
Fe	pmol m ⁻³	14	1464 (113–3537)	3	2356 (1809–2804)
Mn	pmol m ⁻³		–	3	57 (54–63)
Pb	pmol m ⁻³	14	21 (1.6–39)	3	18 (12–27)
Sb	pmol m ⁻³	14	4.0 (0.11–7.5)	3	25 (23–27)
Sc	pmol m ⁻³	12	0.26 (0.065–0.70)	3	0.34 (0.25–0.42)
V	pmol m ⁻³	14	69 (9.0–146)	3	53 (36–64)
Zn	pmol m ⁻³	13	148 (13–299)	3	272 (121–540)
Na ⁺	nmol m ⁻³	14	102 (7.0–241)	3	43 (27–75)
NH ₄ ⁺	nmol m ⁻³	14	101 (22–204)	3	186 (149–212)
K ⁺	nmol m ⁻³	14	3.7 (0.81–8.3)	3	2.9 (1.8–3.8)
Mg ²⁺	nmol m ⁻³	14	12 (0.98–30)	3	6.0 (3.8–10)
Ca ²⁺	nmol m ⁻³	14	5.1 (2.5–13)	3	3.6 (2.6–4.6)
F ⁻	nmol m ⁻³	14	0.21 (0.12–0.38)	3	0.20 (0.13–0.33)
Cl ⁻	nmol m ⁻³	14	102 (8.3–269)	3	28 (16–51)
NO ₃ ⁻	nmol m ⁻³	14	48 (3.3–95)	3	11 (6.5–17)
SO ₄ ²⁻	nmol m ⁻³	14	37 (12–83)	3	50 (33–61)
NSS-SO ₄ ²⁻	nmol m ⁻³	14	31 (4.3–71)	3	48 (31–56)
HCOO ⁻	nmol m ⁻³	14	0.63 (0.21–2.9)	3	2.4 (2.3–56)
CH ₃ COO ⁻	nmol m ⁻³	14	0.46 (0.17–1.8)	3	1.7 (1.5–1.9)
C ₂ H ₅ COO ⁻	nmol m ⁻³	14	0.18 (0.052–0.60)	3	0.29 (0.25–0.32)
CH ₃ SO ₃ ⁻	nmol m ⁻³	14	0.24 (0.017–0.80)	3	0.96 (0.77–1.2)
(COO) ²⁻	nmol m ⁻³	14	4.7 (2.1–9.7)	3	6.1 (4.8–6.9)
CH ₂ (COO) ²⁻	nmol m ⁻³	14	3.4 (1.4–7.1)	3	4.6 (3.8–5.3)
C ₂ H ₄ (COO) ²⁻	nmol m ⁻³	14	5.9 (1.6–15)	3	5.8 (3.3–7.7)

–: Element Mn in 2007 samples was not measured.

^a The concentrations of size-segregated samples in 2008 are the summation of concentrations from all 10 size stages.

^b N is the numbers of valid samples.

(Hopper and Barrie, 1988; Gao et al., 1992; Pike and Moran, 2001). As a major source for anthropogenic V is oil combustion (Nriagu and Pacyna, 1988; Nriagu, 1989; Juichang et al., 1995), lower V concentrations observed at this coastal site may suggest less influence from oil industry than at other coastal regions. However, the concentrations of V at this site were much higher than those over the Atlantic Ocean, for example an average of 2.56 pmol m^{-3} found by Johansen et al. (2000), indicating that this location was more affected by pollution emissions than remote oceanic regions. Similar situations generally existed with other elements in particular Pb, Zn, and Cd: their average concentrations were lower than certain coastal sites (Gao et al., 1992; Pike and Moran, 2001) but higher than in the Atlantic Ocean (Church et al., 1990; Johansen et al., 2000).

For water-soluble ions, NSS-sulfate, ammonium, nitrate, chloride and sodium accounted for up to 70% of the total ions measured in bulk samples, and NSS-sulfate and ammonium were dominant components in the size-segregated samples. The concentrations of NSS-sulfate ranged from 4.3 to 71 nmol m^{-3} in bulk samples and from 31 to 56 nmol m^{-3} in size-segregated samples. NSS-sulfate was positively correlated with MSA (in bulk samples: $R^2 = 0.73$; in size-segregated samples: $R^2 = 0.74$), suggesting that similar ambient conditions may affect their characteristics, although both could come from marine biogenic sources, such as the oxidation of dimethylsulfonate (DMS) (Andreae et al., 1986; Bates et al., 1987; Leck and Rodhe, 1991). Our further data analysis indicated that both NSS-sulfate and MSA had high correlations with temperature and wind speeds with all R^2 values being ~ 0.7 . In addition, both NSS-sulfate and MSA were accumulated in fine-mode particles, and the similar size distributions could also contribute to their high correlations. On the other hand, the mass ratios of NSS-sulfate/MSA ranged from 70 to 479 in bulk samples and from 41 to 60 in size-segregated samples, significantly higher than 19, the average mass ratio in remote oceans (Arimoto et al., 1996; Allen et al., 1997), implying that only a small portion of the NSS-sulfate at this location came from a marine biogenic source. Air-mass back trajectories shown in Fig. 3 confirmed that this location was strongly impacted by air masses of continental origins during the sampling period in this study. The much higher mass ratios in bulk samples indicated stronger anthropogenic fingerprint, which may be caused by more intensive local emissions or more air-mass originated from polluted regions. The concentrations of nitrate in size-segregated samples were lower than those in bulk samples. One possible reason could be the effect of higher ambient temperature in summer during the MOUDI sample collection (Table 1) that could cause the nitrate loss due to evaporation (Schaap et al., 2004). On the other hand, the cellulose filter used in bulk sample collection may result in overestimation of nitrate due to absorption of nitric acid gas (Savoie and Prospero, 1982; Schaap et al., 2004), and this may also contribute to the observed concentration differences between the size-segregated and bulk samples.

The Na/Cl mass ratio in seawater is 0.56 and often serves as an indicator of a marine origin (Broecker and Peng, 1982). The mass ratio of Na/Cl found in bulk samples in this study was 0.65, suggesting that marine aerosol contributed to the total aerosol mass. However, the mass ratio of Na/Cl found in size-segregated samples was 1.0, almost double the seawater ratio and higher than that in bulk samples. The higher Na/Cl ratio observed in size-segregated samples could be attributed to the higher ambient temperature during MOUDI sampling in summer compared with the temperature in March when bulk sample collection took place (Table 1), as higher ambient temperature could promote a larger extent of chloride depletion from aerosol particles. A simple calculation based on the equation in Zhuang et al. (1999) showed that Cl depletion was 44% in bulk samples and 64% in size-segregated samples. These results were consistent with those found by Zhao and Gao (2008a,b) in the same region as this study, that high percentages of chloride loss from aerosols were associated with high ambient temperatures.

Organic acids measured at this location accounted for 8.0–9.0% of the total ionic mass (the sum of all anions and cations measured), and

among them succinate, oxalate and malonate were the major components, accounting for 90% of the total mass of organic acids. This was different from both urban and rural areas, where the concentrations of dicarboxylic acids are lower (Falkovich et al., 2005; Zhao and Gao, 2008) and oxalate is the dominant species followed by malonate and succinate (Kawamura et al., 1995, 1996; Khwajia, 1995; Pakkanen et al., 2001; Falkovich et al., 2005; Zhao and Gao, 2008). Organic acids could come from both biogenic (Keene and Galloway, 1986; Talbot et al., 1988; Fehsenfeld et al., 1992) and anthropogenic emissions (Kawamura et al., 1985; Kawamura and Kaplan, 1987; Talbot et al., 1988). The higher concentrations of organic acids observed at this location may imply the influence of the coastal salt marsh ecosystem, where the estuarine plants and soils might be sources of certain organic acids (Mucha et al., 2005; Sannigrahi et al., 2005; Graber and Rudich, 2006; Duarte et al., 2007). As organic acids play significant roles in atmospheric chemistry (Chebbi and Carlier, 1996; Warneck, 2003), such as affecting metal solubility through complexation (Faust and Zepp, 1993; Xu and Gao, 2008), more investigations are needed for a better understanding of organic acids in the chemistry of the coastal marine atmosphere.

3.2. Enrichment factors

As a first step of source identification for certain trace elements, enrichment factor analysis was used to distinguish trace metals from crustal and non-crustal sources and marine and non-marine sources (Zoller et al., 1974; Duce et al., 1975). Crustal abundance from Taylor and McLennan (1985) was used as a reference, with Al being the crustal tracer. By convention, a crustal Enrichment Factor (EF) value of < 10 was taken as an indication that a trace metal in an aerosol has a significant crustal source, whereas a crustal EF value of > 10 was considered to indicate that a significant proportion of an element has a non-crustal source (Chester et al., 1999). The same rule applied to the oceanic EF with sodium as the oceanic tracer and the oceanic abundance from Kaye and Laby (1986).

Fig. 5 shows the enrichment factors for both bulk and size-segregated samples. The results indicated that the patterns of aerosol elemental composition at this location were constant relative to the crustal source strength, although the aerosol samples were collected in different years. Aluminum, Sc, Fe, K, Ca, and Co can be grouped as crustal elements, and Cu, V, Na, Pb, Zn, Sb, Cd were non-crustal elements. However, EFs of most trace metals were higher for the bulk samples than those for size-segregated samples. Particularly the median values of crustal EFs of Na, Mg, K, and Ca were higher in bulk samples than those in size-segregated samples, and this may partly be due to the differences in wind directions during the sampling periods between 2007 and 2008. As shown in Fig. 2, stronger winds from the ocean sectors occurred in

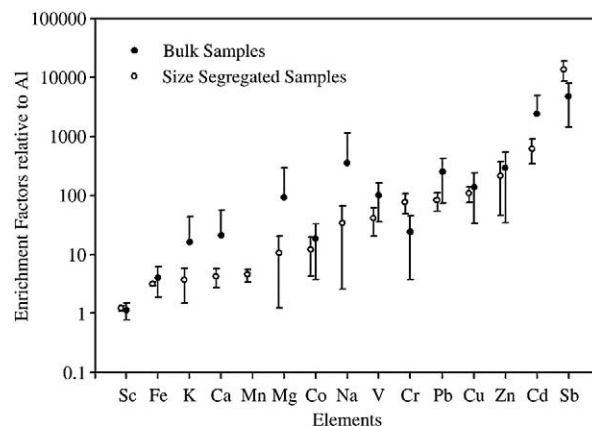


Fig. 5. Crustal enrichment factors of bulk and size-segregated samples with standard deviation.

2007 that could bring in more influences of marine source during bulk sample collection. On the other hand, the winds from the inland directions were also stronger in 2007 than in 2008, which could explain the fact that V, Pb and Cd in bulk samples were more enriched in 2007, indicating the influences of anthropogenic sources such as heavy oil combustions (Nriagu and Pacyna, 1988). The elements, Cr and Sb, showed higher EFs in size-segregated samples, attributed to their enrichment in fine-mode particles, which contributed 78% of Cr EFs and 88% of Sb EFs. These two elements could be derived primarily from coal combustion, sewage sludge incineration (Nriagu and Pacyna, 1988) and vehicular traffic (Iijima et al., 2008). Therefore, the varying strength of different sources may contribute to the different EFs.

3.3. Mass-size distributions

The mass-size distributions of the three MOUDI samples showed typical bi-modal distributions (Fig. 6). The first peak was at 0.18–0.56 μm , accounting for 70–80% of the total mass concentration. However, the second peaks in the three sample sets were different: the second peak for the first set was at 1.0–3.2 μm , and ranged from 3.2 to 5.6 μm for the second and third sets. The size distribution patterns at this site are similar to those measured at an urban site in the same region (Zhao and Gao, 2008), although the total mass concentrations at this coastal site were almost 10 times less than that in the urban area. Total mass-size distributions were contributed by different species, and each species contributed differently in the fine and coarse modes. In this work, 1.0 μm was used as the cut-off size to separate the fine and coarse particles. In fine particles, NSS-sulfate and ammonium were the major components, accounting for 79% of the total mass of PM_{1.0} (particulate matter with a diameter less than 1.0 μm). This was different from results from urban areas, where sulfate and nitrate were dominant components (Zhuang et al., 1999; He et al., 2001; Lin, 2002; Zhao and Gao, 2008). On the other hand, dicarboxylic acids, mainly oxalate and succinate, were secondary major components at this location, accounting for 13% of the total fine particle mass, which was much higher than that in the urban area ($1.9 \pm 0.9\%$) (Zhao and Gao, 2008). As the C2–C4 dicarboxylic acids are relatively abundant in remote oceanic regions (Mochida et al., 2003; Kawamura et al., 2007), they could be common in coastal areas as well. Possibly, the wide salt marsh ecosystem in the study region could be another source of organic acids.

In coarse particles, Na and Cl were major contributors, followed by nitrate and minor sea-salt sulfate. Coarse Na and Cl were mainly from sea-salt spray (Harrison and Pio, 1983; Herner et al., 2006) and coarse-mode nitrate was mainly formed through the reactions of nitric acid onto existing coarse particles, such as sea salt (Wu and Okada, 1994; Pakkanen, 1996; Anlauf et al., 2006). In addition, Zhao and Gao (2008a) found that temperature could affect size distributions of nitrate, resulting in the shift of the dominant nitrate peak from

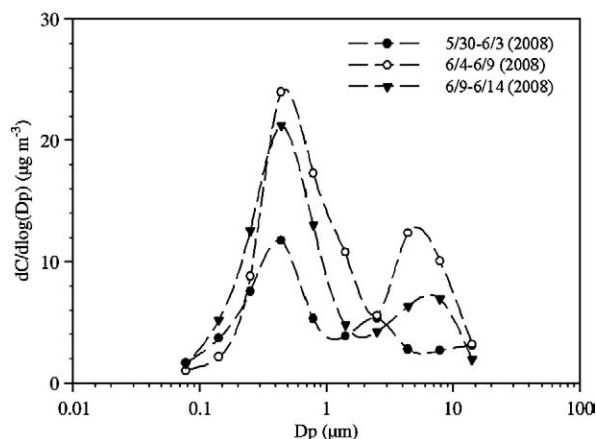


Fig. 6. Total aerosol mass-size distributions of three set MOUDI samples.

fine mode to coarse mode when the temperature is higher than 17 °C. Observations at this location were consistent with the above result. During MOUDI sample collection, the ambient average temperatures for all three samples were above 19 °C, and the dominant peaks for nitrate in these samples appeared in coarse mode, suggesting that high temperature may promote the formation of coarse-mode nitrate.

Chemical components from different sources may display different mass-size distributions. Sodium is a typical element in marine aerosols, showing mass accumulation in the coarse mode (Fig. 7a), consistent with previous studies (Li-Jones and Prospero, 1998). The dominant peaks for Na were at 1.8–3.6 μm for set one, and 3.6–5.6 μm for sets two and three, and the same patterns were found for Cl (Fig. 7b). Sodium and chloride were the major contributors to the coarse mode, and their distribution patterns controlled the total mass-size distributions. In addition to sea salts, Na and Cl could also come from anthropogenic emissions such as waste incineration (Kaneyasu et al., 1999) and secondary aerosol formation processes (Spurny, 2000), but there was little indication of anthropogenic influence on Na and Cl based on the observed size distributions of both elements.

Iron and aluminum, as typical crustal elements, were found to have multiple peaks at this location (Fig. 7c and d). The size distributions of Fe were bi-modal, with the major peak ranging from 3.6 to 5.6 μm , and the minor peak at 0.36–0.56 μm , consistent with previous work (Infante and Acosta, 1991; Lyons et al., 1993; Horvath et al., 1996; Allen et al., 2001). The percentages of Fe mass concentrations in coarse mode in each of three MOUDI sample were 68%, 54% and 63%, respectively. Iron in the coarse mode is mainly derived from soil or road dust, and its fine particles can originate from anthropogenic emissions, such as fly ash (Gao et al., 2007; Anderson and Hua, 2008). Aluminum showed four peaks at 0.056 μm , 0.18–0.32 μm , 0.56–1.0 μm , and 3.2–5.6 μm , with the coarse mode accounting for ~68–84% of the total Al mass in all three samples. Aluminum in the coarse mode is mainly of crustal origin, and its fine mode could come from different anthropogenic sources, such as motor vehicles (Kleeman et al., 2000) and metallurgical activities and coal combustion (Gao et al., 1997; Hlavay et al., 1998). Hence, chemical components consisting of both coarse and fine modes could originate from both crustal and anthropogenic sources.

Nitrate accumulated in the coarse mode with a small peak in the fine fraction (Fig. 7e). The formation of coarse-mode nitrate could be from the reaction of HNO₃ or NO_x with coarse particles, such as sea salt (Wu and Okada, 1994; Pakkanen, 1996; Anlauf et al., 2006). This reaction could be the major formation pathway for nitrate in coastal areas (Zhuang et al., 1999). This mechanism was supported by the similar mass-size distribution patterns of Na and nitrate observed at this location. The minor peak at 0.32–0.56 μm for nitrate could be caused by the involvement of Ca with nitrate, as the minor peak of Ca overlapped with the nitrate peak. Anthropogenic NSS-sulfate was calculated by total NSS-sulfate minus DMS source NSS-sulfate (DMS source NSS-sulfate = MSA × 19) (Arimoto et al., 1996), and it showed a dominant mode at 0.36–0.56 μm (Fig. 7f). The formation of submicrometer NSS-sulfate results from gas-particle conversion reactions (Charlson et al., 1987; Li-Jones and Prospero, 1998) and in-cloud processes (John et al., 1990; Meng and Seinfeld, 1994; Kerminen and Wexler, 1995).

3.4. Fe characteristics

The Fe_T concentrations observed at this location ranged from 113 to 3537 pmol m⁻³. They were lower than other US East Coast areas, such as New Castle, NH, US (Pike and Moran, 2001), and were also lower than open ocean where the dust influence is strong (Table 3) (Church et al., 1990; Buck et al., 2006, 2008a,b), suggesting that the dust influence at this location was low. The Fe(II)s concentrations from bulk samples ranged from 50 to 518 pmol m⁻³, and were higher than open ocean regions in general (Table 3). In addition, Fe solubility observed ranged from 11% to 44% with an average of 18%, higher than reported results from oceanic regions (Baker et al., 2006; Sedwick

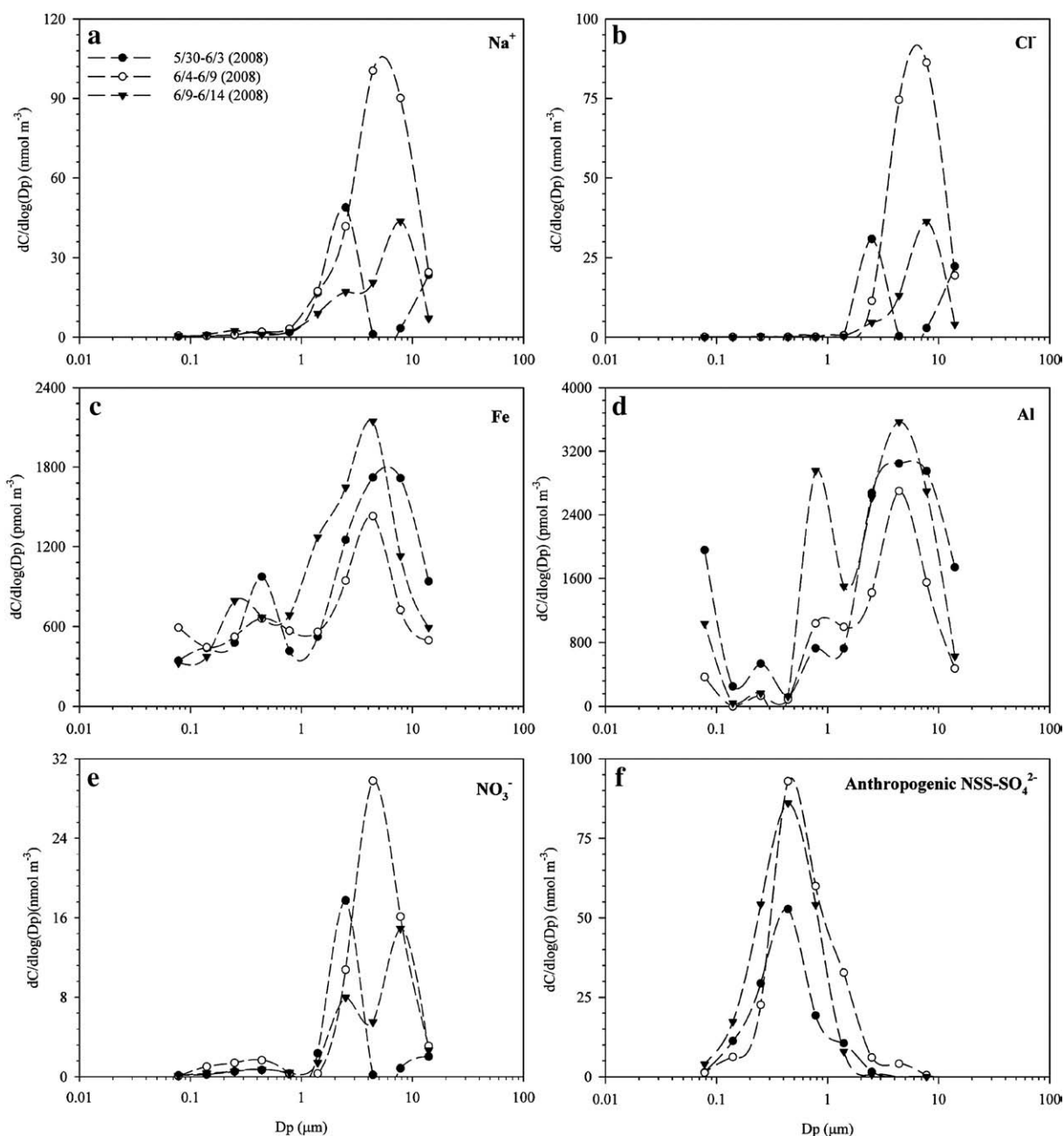


Fig. 7. Mass-size distributions of different chemical components: (a) Na; (b) Cl; (c) Fe; (d) Al; (e) nitrate (f) anthropogenic NSS-sulfate, calculated by NSS-sulfate minus DMS source NSS-sulfate, and DMS source NSS-sulfate concentration was calculated from the mass ratio of NSS-sulfate/MSA (Arimoto et al., 1996).

et al., 2007; Buck et al., 2008a,b) (Table 3). Therefore, the relatively high iron solubility and low iron concentrations observed at this site suggest that anthropogenic emissions are more important than dust to affect atmospheric Fe in this region. A number of factors may contribute to Fe solubility, such as particle size, interaction with certain acidic components, etc. (Spokes and Jickells, 1996; Jickells and Spokes, 2001; Desboeufs et al., 2001), and we briefly discuss some of them below based on the results found at this location.

3.4.1. Effect of aerosol particle size

Aerosol particle size may play an important role in controlling Fe solubility (Baker and Jickells, 2006; Buck et al., 2008b; Ooki et al., 2009). In this study, Fe solubility was higher in the fine mode than that in the coarse mode (Fig. 8), consistent with previous observations (Siefert et al., 1999; Johansen et al., 2000; Chen and Siefert, 2004; Baker and Jickells, 2006; Ooki et al., 2009). The high and low values of Fe solubility

were clearly separated by the 1.0 μm cut-off diameter, with fine particles having solubility higher than 50% and coarse particle solubility less than 20%. In addition, the concentration of Fe(II)s in fine-mode particles accounted for ~60% of the total Fe(II)s.

The high Fe solubility was primarily associated with the low Fe_T concentrations ($<1000 \text{ pmol m}^{-3}$) as shown in Fig. 9a, consistent with other studies (Buck et al., 2006; Sedwick et al., 2007; Sholkovitz et al., 2009), although some of these studies did not conclude with a simple inverse relationship between Fe_T load and Fe solubility in aerosols (Buck et al., 2008b). The observed relationship between Fe solubility and Fe_T concentration in this study could be the result of different particle sizes affected by different aerosol sources. Fe of anthropogenic origin could be associated more with fine particles and have higher solubility (Guieu et al., 1997; Jickells and Spokes, 2001; Johnson, 2001; Sedwick et al., 2007; Sholkovitz et al., 2009). Our results of EFs calculations (Fig. 5) clearly demonstrated that the

Table 3
Comparison of Fe_T concentrations, Fe(II)s concentrations and Fe solubility in different locations.

Locations	Fe_T (pmol m^{-3})	Fe(II)s (pmol m^{-3})	Fe(II)s/Fe_T (%)	Leaching pH	Citations
North Pacific	180–2680	90–2410	11–100	<1.0	Zhuang et al. (1992a, b)
	170–1370	0.70–95	0.1–4.5	8.1	Buck et al. (2006)
			0.10–0.91 ^a	DI water	Chuang et al. (2005)
North Atlantic	10,700–89,280	500–2680	34–64	<1.0	Zhuang et al. (1992a, b)
	437–15,000	11–150	0.20–6.5	1.0	Zhu, et al. (1997)
	29–17,600	2.1–304	0.30–5.1	4.5	Chen and Siefert (2004)
	25–74,643		1.0–26 ^a	5.6	Buck et al. (2008a)
	50–27,804		0.4–19 ^a	5.5	Sedwick et al. (2007)
	946–42,500	17.5–91	0.05–2.4	4.2	Johansen et al. (2000)
Indian Ocean	100–1600		1.4–54 ^a	4.7	Baker et al. (2006)
		<1.6–84	<4.0	4.2	Siefert et al. (1999)
Urban		2140–3750	4.0–11	<1.0	Zhuang et al. (1992a,b)
		320–380	4.6	4.3	Majestic et al. (2006)
US East Coast	113–3537	50–518	11–44	1.0	This work

^a Fe solubility = 100 total soluble Fe/Fe_T .

aerosol mass at this location was impacted by a variety of pollution sources. In addition, long range transport may carry fine-mode particles to a long distance while coarse-mode particles may settle along the transport pathway (McTainsh and Walker, 1982; Duce et al., 1991). As shown in Fig. 3, with the air-mass transport distances being at least 2400 km, the residence time of these small aerosols in the atmosphere was relatively long before being sampled and that could be in favor of fine-mode particle accumulation. Therefore, the lower concentration of aerosol mass, corresponding to the lower concentration of Fe_T , may contain more fine particles and consequently show higher Fe solubility. However, there were several exceptions found in this study. For example, the last stage (0.056 μm) of the second set of MOUDI samples showed low Fe_T loading (150 pmol m^{-3}) as well as relatively low Fe solubility (17%) (Fig. 9b). Similar results were also reported in some studies (Chen and Siefert, 2004; Buck et al., 2008b). This may indicate that, besides particle size, other factors may also control Fe solubility, such as mineralogy (Journet et al., 2008) or surface reactions with other air components, such as sulfate and oxalate.

3.4.2. Effect of inorganic acidic components

An acidic environment can enhance Fe solubility in aerosols (Zhu et al., 1992; Spokes et al., 1994). However, measuring aerosol acidity is challenging, and several indicators have been used to address this issue, such as NSS-sulfate or nitrate (Chen and Siefert, 2004; Buck et al., 2006, 2008a), molar ratio of ammonium to NSS-sulfate (Hand et al., 2004), and potential acidity (Baker et al., 2006). In this study, the molar ratio of NSS-sulfate to Fe_T was used as an acidity indicator to explore the effect of the acidity of NSS-sulfate on Fe solubility, since NSS-sulfate is the major inorganic acidic species in aerosols. Fig. 10a

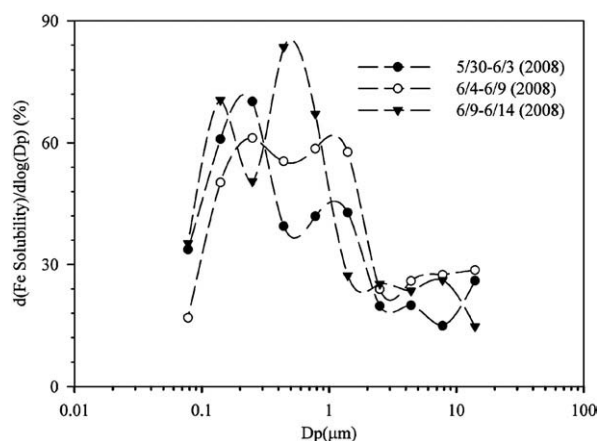


Fig. 8. Size distributions of Fe solubility.

and b showed positive correlations between Fe solubility and molar ratio of NSS-sulfate to Fe_T in both bulk and size-segregated samples. However, NSS-sulfate acidity could be neutralized by basic species, such as ammonium. In both bulk and size-segregated samples, the average molar ratios of ammonium to NSS-sulfate were higher than

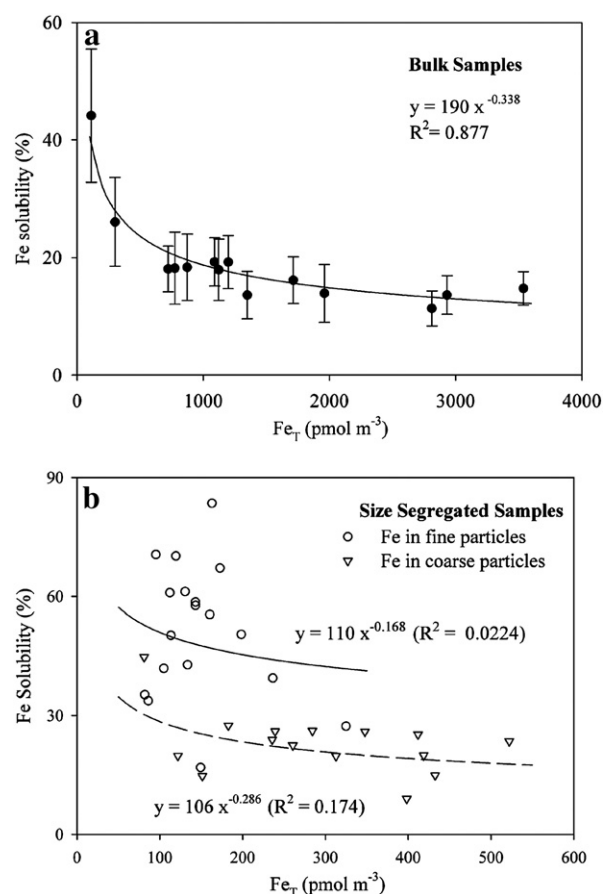


Fig. 9. Correlations between Fe solubility and Fe_T concentration: (a) correlation in bulk samples (The plot included the high point (113 pmol m^{-3} , 44%); if without that point, the plot's R^2 is 0.76 and the equation is $y = 50.053 x^{-0.275}$). The averaged Fe solubility in bulk samples is 19% with standard deviation of 8.1%; (b) correlation in size-segregated samples. The Fe solubility uncertainties of bulk samples plotted on (a) were calculated by the summation of sampling uncertainty (10%), Fe(II)s measurement uncertainty (four time repeated measurement for each), and Fe_T measurement uncertainty (2.1%). The Fe solubility uncertainties of size-segregated samples were not plotted on (b), as the limitation of filters, every sample has the same uncertainty (24% = sampling uncertainty (5%) + Fe(II)s measurement uncertainty (14%) + Fe_T measurement uncertainty (5.3%).

2.0, indicating that NSS-sulfate has been totally neutralized (Pathak et al., 2004; Hand et al., 2004). Therefore, the positive correlations between Fe solubility and molar ratio of NSS-sulfate to Fe_T may reflect that interaction with more NSS-sulfate during aerosol transport could transfer more Fe into soluble species, rather than indicate the relationship between aerosol acidity and Fe solubility during sampling periods.

3.4.3. Effect of oxalate

The molar ratios of oxalate to Fe_T also showed a positive correlation with Fe solubility for bulk and size-segregated samples (Fig. 10c and d). The highest value of the oxalate to Fe_T molar ratio in bulk samples was from the sample collected on March 16th from 9:00 to 17:00, when a precipitation event took place. Fe_T concentrations decreased from 873 pmol m^{-3} during the previous night to 113 pmol m^{-3} on this day, while oxalate concentration increased from 2.1 nmol m^{-3} for the previous night to 7.4 nmol m^{-3} on this day. As the concentration of certain species also increased during this precipitation event, such as malonate from 2.2 to 5.3 nmol m^{-3} , we considered the Fe concentration during this period not to be an outlier. This positive correlation between Fe solubility and oxalate to Fe_T molar ratio may be caused by the influence of oxalate on Fe solubility (Jickells and Spokes, 2001; Xu and Gao, 2008) through photoreactive complexation (Zuo and Hoigné, 1992; Erel et al., 1993; Pehkonen et al., 1993; Sedlak and Hoigné, 1993; Saydam and Senyuva, 2002; Kieber et al., 2005). The correlation observed in this work is comparable with the result from Chen and Siefert (2004), although a similar correlation was not observed in other studies (Buck et al., 2008a). In size-segregated samples, coarse particles have a lower

oxalate concentration as well as lower Fe solubility compared with those associated with fine particles. However, due to limited number of size-segregated samples in this study, the detailed relationship between oxalate and Fe solubility needs further investigation.

3.4.4. Effect of photochemical reactions

Results from samples separately collected between day and night in 2007 showed that the Fe(II)s concentrations varied slightly between these two periods (Fig. 11a), with the Fe(II)s concentration being slightly lower during nighttime compared with that in the following daytime samples. However, Fe(II)s showed the same concentration variation as did Fe_T (Fig. 11c). Thus the “diel” change of Fe(II)s concentration between nighttime and the following daytime could be caused by the continuous increase and accumulation of Fe_T as well as total aerosol concentration. The diel variation of Fe solubility may occur during photochemical processes that transfer Fe(III) to Fe(II) and increase Fe solubility (Zuo and Hoigné, 1992; Pehkonen et al., 1993; Siefert et al., 1994; Zuo, 1995; Saydam and Senyuva, 2002). However, this pattern has not been observed at this location (Fig. 11b). Previous field works were not consistent with one another. Zhu et al. (1997) reported this diel variation of Fe solubility at Barbados, while in the Pacific Ocean no similar trend was found (Buck et al., 2006). In Fig. 10c and d, Fe solubility varied along with oxalate/ Fe_T , with higher Fe solubility associated with higher molar ratios of oxalate to Fe_T in the fine fraction. Therefore, as discussed in Section 3.4.3, the existence of oxalate in this study may play an important role in controlling Fe solubility through photochemical reactions (Kieber et al., 2005).

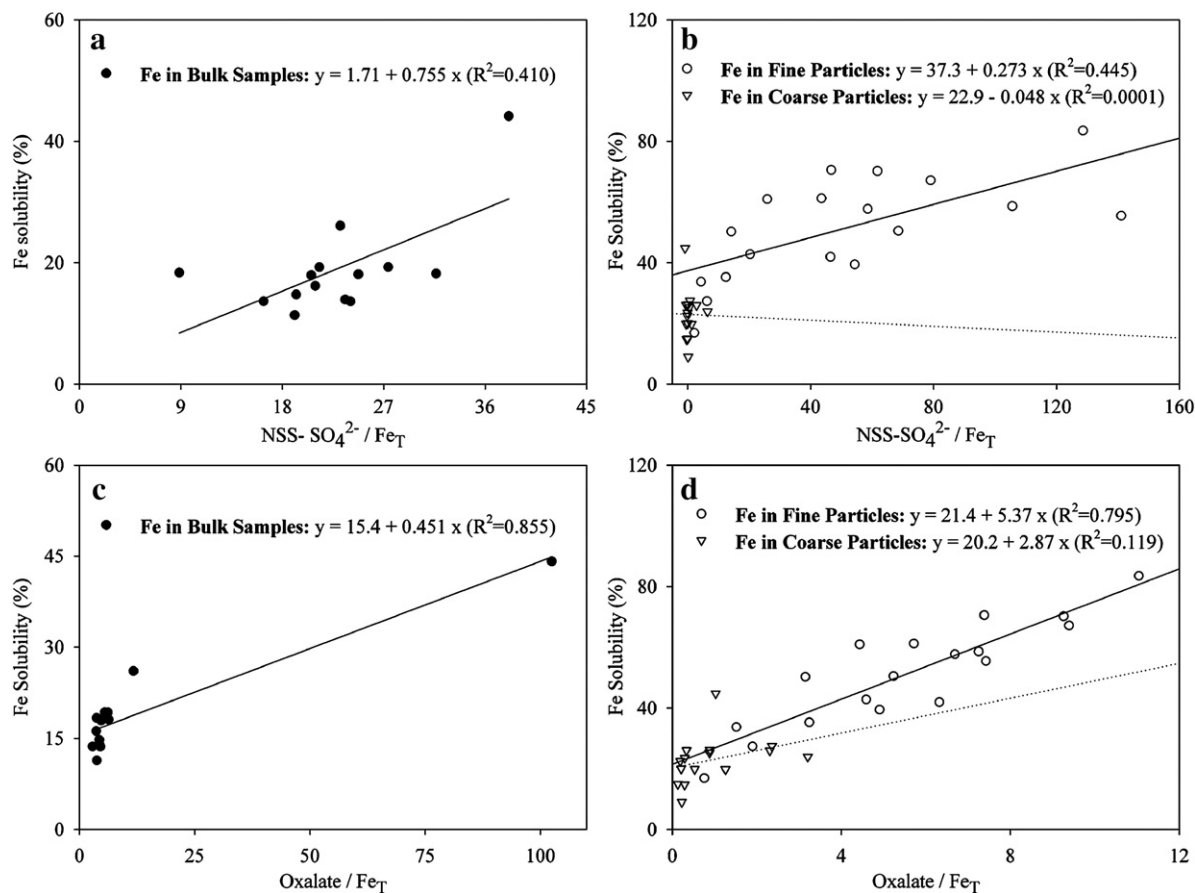


Fig. 10. Inorganic and organic acidic components effecting Fe solubility: (a) and (b) correlations between Fe solubility and the molar ratio of NSS-sulfate to Fe_T concentration; and (c) and (d) correlations between Fe solubility and the molar ratio of oxalate to Fe_T (in c, without the highest Fe solubility point, $R^2 = 0.735$). In (b) and (d), the solid lines are linear regression of fine particles, and the dash-dot lines are linear regression of coarse particles.

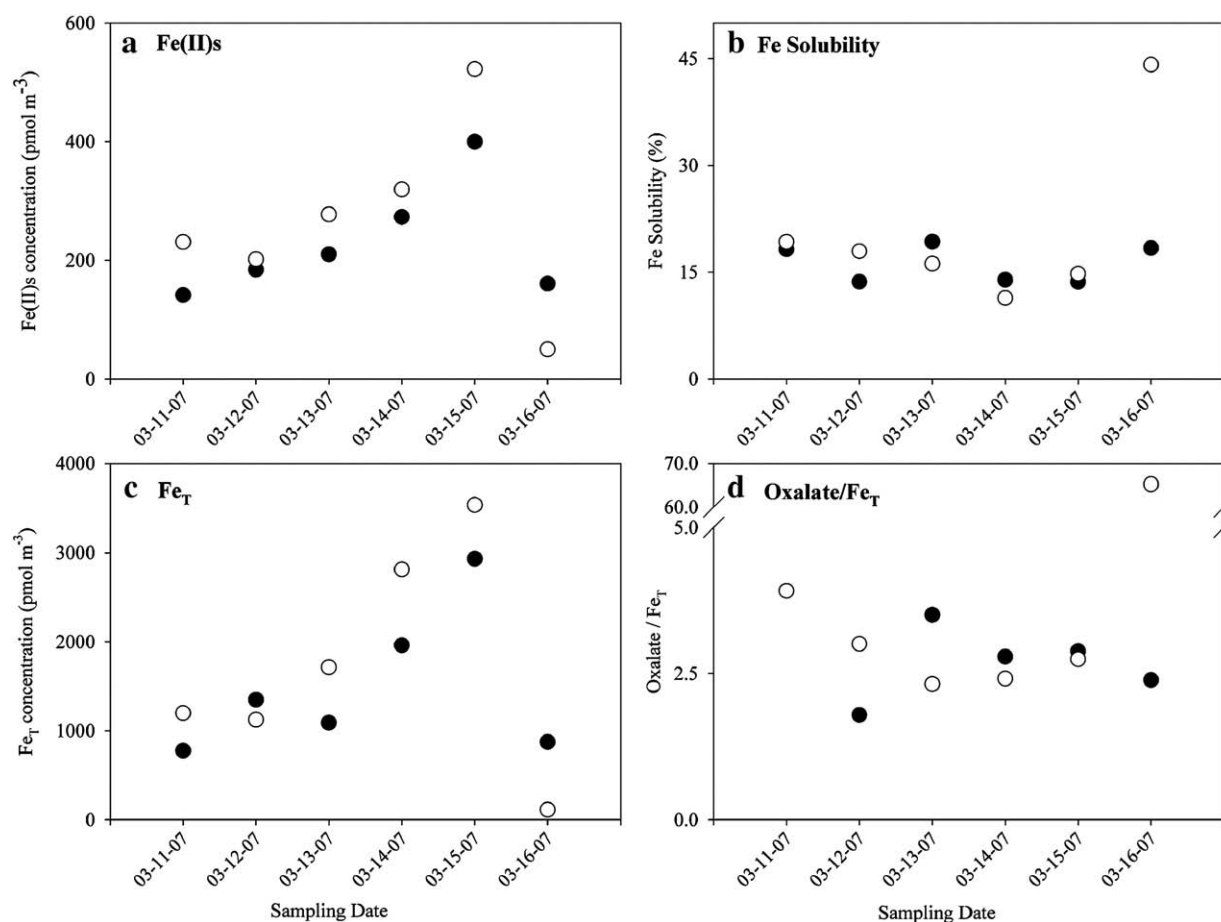


Fig. 11. The diel variation (N is night and D is day) before March 16th: (a) Fe_T concentration and Fe(II)s concentration; (b) Fe solubility and the ratio of oxalate to Fe_T.

3.4.5. Effect of anthropogenic emissions

Anthropogenic emissions may enhance Fe solubility (e.g. Chuang et al., 2005). There could be two ways to increase Fe solubility: more soluble Fe is emitted directly from anthropogenic sources, and Fe in aerosols interacts with anthropogenic pollutants, increasing its solubility. To investigate the first possibility, crustal EF_{Fe} of Fe were used to explore the extent of anthropogenic influence on atmospheric Fe solubility. Fig. 12a showed no significant correlations between Fe solubility and EF_{Fe} in both bulk and size-segregated samples. For bulk samples, when EF_{Fe} changed from 1.2 to 9.5, the Fe solubility only increased from 11.4% to 13.6%. In size-segregated samples, although more fine particles showed high Fe solubility, their EF_{Fe} varied in a broad range from 1.1 to 43. In this study, V normalized by Al was also used as an indicator of anthropogenic emissions (Sedwick et al., 2007; Sholkovitz et al., 2009). However, the ratios of 100 V/Al in both bulk and size-segregated aerosol samples did not show correlations with Fe solubility (Fig. 12b) as strong as they were found by Sholkovitz et al. (2009), suggesting that the ambient atmospheric system is more complicated at this location. The low correlations between V/Al and Fe solubility in aerosols found in this study may suggest that anthropogenic emissions are not a direct major source of Fe solubility enhancement at this location, although Fe from anthropogenic emissions is more easily exchangeable than in mineral dust (Chester et al., 1993; Spokes et al., 1994; Guieu et al., 1997). However, as the atmospheric system is complex, and correlation is not a cause-and-effect relationship, there might be other mechanism to cause the low correlation. On the other hand, based on higher correlations between the molar ratio of NSS-sulfate to Fe_T and Fe solubility (Fig. 10a and b) than the ones between V/Al and Fe solubility, the anthropogenic influence on Fe solubility may be more efficient through the interac-

tions of Fe with acidic air pollutants, possibly through heterogeneous and cloud processes.

4. Conclusion

The major components in coastal aerosols at this location were NSS-sulfate, nitrate, ammonium, sodium and chloride, accounting for ~70% of the total mass, followed by dicarboxylic acids, accounting for ~10% of the total mass. NSS-sulfate, ammonium and dicarboxylic acids were mainly associated with fine-mode particles and nitrate, sodium and chloride were associated with the coarse mode. Because of their dominant roles in aerosol total mass, they significantly controlled the mass concentration and mass-size distribution of coastal aerosols.

Aerosols at this location showed a typical bi-modal mass-size distribution with the major peak ranging from 0.36 μm to 0.56 μm and a minor one in the coarse mode. Two fold higher aerosol mass concentrations in the fine mode, compared with the coarse mode, may indicate a strong anthropogenic effect from adjacent urban areas. The total mass-size distribution was a result of different individual components. Elements from the ocean, such as sodium and chloride and from the crust, such as Al and Fe, showed a major peak in the coarse mode. Trace metals from anthropogenic emissions, such as V and Sb, were mainly associated with fine-mode particles. On the other hand, components which could be in the gas phase or be active in gas-aqueous reactions, such as sulfate and nitrate, could be associated with both fine and coarse particles, depending on the initial aerosol properties and atmospheric environment.

Iron solubility at this location was ~18% in bulk samples and ranged from 9.0% to 84% in size-segregated samples. Soluble Fe in aerosols over

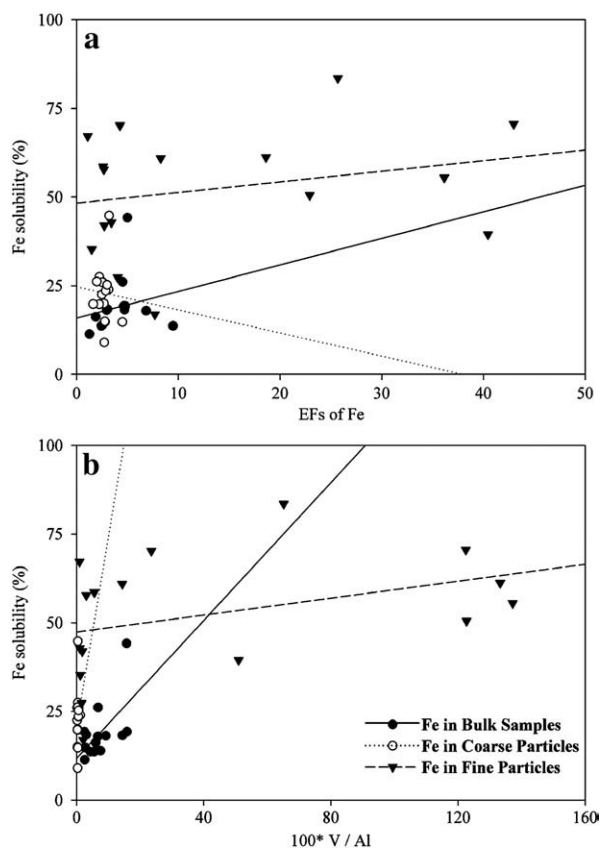


Fig. 12. (a) Correlations between Fe solubility and EFs of Fe in both bulk samples (solid line: $y = 15.9 + 0.749x$, $R^2 = 0.0399$) and size-segregated samples (dash-dot line is coarse particles: $y = 24.7 - 0.651x$, $R^2 = 0.0029$, and dashed line is fine particles: $y = 48.3 + 0.299x$, $R^2 = 0.0650$); (b) correlations between Fe solubility and $100 V / Al$ in both bulk samples (solid line: $y = 11.8 + 0.971x$, $R^2 = 0.327$) and size-segregated samples (dash-dot line is coarse particles: $y = 20.6 + 5.34x$, $R^2 = 0.0286$, and dashed line is fine particles: $y = 47.3 + 0.119x$, $R^2 = 0.138$).

coastal regions may contribute to the soluble Fe input to the downwind North Atlantic Ocean. High Fe solubility was correlated with fine particles and low Fe_T concentrations and associated with high molar ratios of NSS-sulfate to Fe_T and oxalate to Fe_T , indicating that particle size, aerosol acidity and organic components may have a strong impact on Fe solubility. Anthropogenic emissions may also strongly influence Fe solubility through interactions with acidic air pollutants.

Acknowledgments

This work is supported by NASA Ocean Biology and Biogeochemistry Program (Award #NNG04G091G). We sincerely thank Dr. Kenneth Able and staff at Rutgers University Tuckerton Marine Field Station for support on field operation. Our appreciation also goes to Fei Song, Rafael Jusino and Christopher Thuman for sampling assistance and useful discussions. We gratefully acknowledge the constructive comments from two anonymous reviewers that helped us significantly improve this paper.

References

Allen, A.G., Dick, A.L., Davidson, B.M., 1997. Sources of atmospheric methanesulphonate, non-sea-salt sulphate, nitrate and related species over the temperate South Pacific. *Atmospheric Environment* 31 (2), 191–205.

Allen, A.G., Nemitz, E., Shi, J.P., Harrison, R.M., Greenwood, J.C., 2001. Size distributions of trace metals in atmospheric aerosols in the United Kingdom. *Atmospheric Environment* 35, 4581–4591.

Anderson, J.R., Hua, X., 2008. Coal ash aerosol in East Asian outflow as a source of oceanic deposition of iron and other metals. EOS, Transactions, American Geophysical Union, Fall meeting, Abstract OS13F-01.

Andreae, M.O., et al., 1986. Internal mixture of sea salt, silicates, and excess sulfate in marine aerosols. *Science* 232 (4758), 1620–1623.

Anlauf, K., et al., 2006. Ionic composition and size characteristics of particles in the Lower Fraser Valley: Pacific 2001 field study. *Atmospheric Environment* 40 (15), 2662–2675.

Arimoto, R., Duce, R.A., Ray, B.J., Ellis, W.G., Cullen, J.D., Merrill, J.T., 1995. Trace elements in the atmosphere over the North Atlantic. *Journal of Geophysical Research* 100 (D1), 1199–1213.

Arimoto, R., et al., 1996. Relationships among aerosol constituents from Asia and the North Pacific during PEM-West A. *Journal of Geophysical Research* 101, 2011–2023.

Baker, A.R., Jickells, T.D., 2006. Mineral particle size as a control on aerosol iron solubility. *Geophysical Research Letters* 33, L17608.

Baker, A.R., Jickells, T.D., Witt, M., Linge, K.L., 2006. Trends in the solubility of iron aluminium, manganese and phosphorus in aerosol collected over the Atlantic Ocean. *Maine Chemistry* 98, 43–58.

Barbeau, K., Rue, E.L., Bruland, K.W., Butler, A., 2001. Photochemical cycling of iron in the surface ocean mediated by microbial iron(III)-binding ligands. *Nature* 413, 409–413.

Bates, T.S., Cline, J.D., Gammon, R.H., Kelly-Hansen, S.R., 1987. Regional and seasonal variations in the flux of oceanic dimethylsulfide to the atmosphere. *Journal of Geophysical Research* 92, 2930–2938.

Brock, C.A., et al., 2008. Sources of particulate matter in the northeastern United States in summer: 2. Evolution of chemical and microphysical properties. *Journal of Geophysical Research* 113, D08302.

Broecker, W.S., Peng, T.-H., 1982. *Tracers in the Sea*. Eldigio Press, Palisades, NY.

Buck, C.S., Landing, W.M., Resing, J.A., Lebon, G.T., 2006. Aerosol iron and aluminum solubility in the northwest Pacific Ocean: results from the 2002 IOC cruise. *Geochemistry Geophysics Geosystems* 7, 1–21.

Buck, C.S., Landing, W.M., Resing, J.A., Measures, C.I., 2008a. The solubility and deposition of aerosol Fe and other trace elements in the North Atlantic Ocean: observations from the A16N CLIVAR/CO2 repeat hydrography section. *Marine Chemistry*. doi:10.1016/j.marchem.2008.08.003.

Buck, C.S., Landing, W.M., Resing, J.A., 2008b. Particle size and aerosol iron solubility: a high-resolution analysis of Atlantic aerosols. *Marine Chemistry*. doi:10.1016/j.marchem.2008.11.002.

Castanho, A.D.A., et al., 2005. Chemical characterization of aerosols on the East Coast of the United States using aircraft and ground-based stations during the CLAMS experiment. *Journal of the Atmospheric Sciences* 62 (4), 934–946.

Charlson, R.J., Lovelock, J.E., Andreae, M.O., Warren, S.G., 1987. Oceanic phytoplankton, atmospheric sulphur, cloud albedo and climate. *Nature* 326, 655–661.

Chebbi, A., Carlier, P., 1996. Carboxylic acids in the troposphere, occurrence, sources and sinks: a review. *Atmospheric Environment* 30, 4233–4249.

Chen, Y., Siefert, R., 2004. Seasonal and spatial distributions and dry deposition fluxes of atmospheric total and labile iron over the tropical and subtropical North Atlantic Ocean. *Journal of Geophysical Research* 109, D09305.

Chester, R., et al., 1993. Factors controlling the solubilities of trace metals from non-remote aerosols deposited to the sea surface by the “dry” deposition mode. *Marine Chemistry* 42, 107–126.

Chester, R., Nimmo, M., Proston, M.R., 1999. The trace metal chemistry of atmospheric dry deposition samples collected at Cap Ferrat: a coastal site in the Western Mediterranean. *Marine Chemistry* 68, 15–30.

Chuang, P.Y., Duvall, R.M., Shafer, M.M., Schauer, J.J., 2005. The origin of water soluble particulate iron in the Asian atmospheric outflow. *Geophysical Research Letters* 32, L07813.

Church, T.M., et al., 1990. Trace elements in the North Atlantic troposphere, shipboard results of precipitation and aerosols. *Global Biogeochemical Cycles* 4 (4), 431–443.

Cutter, G.A., 1993. Metalloids in wet deposition on Bermuda: concentrations, sources, and fluxes. *Journal of Geophysical Research* 98 (D9), 16,777–16,786.

de Gouw, J.A., et al., 2005. Budget of organic carbon in a polluted atmosphere: results from the New England air quality study in 2002. *Journal of Geophysical Research* 110, D16305.

Desboeufs, K.V., Losno, R., Colin, J.L., 2001. Factors influencing aerosol solubility during cloud processes. *Atmospheric Environment* 35, 3529–3537.

Doney, S.C., et al., 2007. Impact of anthropogenic atmospheric nitrogen and sulfur deposition on ocean acidification and the inorganic carbon system. *PNAS* 104 (37), 14580–14585.

Duarte, R.M.B.O., Santos, E.B.H., Pio, C.A., Duarte, A.C., 2007. Comparison of structural features of water-soluble organic matter from atmospheric aerosols with those of aquatic humic substances. *Atmospheric Environment* 41, 8100–8113.

Duce, R.A., Tindale, N.W., 1991. Atmospheric transport of iron and its deposition in the ocean. *Limnology and Oceanography* 36, 1715–1726.

Duce, R.A., Hoffman, G.L., Zoller, W.H., 1975. Atmospheric trace metals at remote northern and southern hemisphere sites: pollution or natural? *Science* 187 (4171), 59–61.

Duce, R.A., et al., 1991. The atmospheric input of trace species to the world ocean. *Global Biogeochemical Cycles* 5, 193–259.

Erel, Y., Pehkonen, S.O., Hoffman, M.R., 1993. Redox chemistry of iron in fog and stratus clouds. *Journal of Geophysical Research* 98, 18423–18434.

Falkovich, A.H., et al., 2005. Low molecular weight organic acids in aerosol particles from Rondonia, Brazil, during the biomass-burning, transition and wet periods. *Atmospheric Chemistry and Physics* 5, 781–797.

Falkowski, P.G., Barber, R.T., Smetacek, V., 1998. Biogeochemical controls and feedbacks on ocean primary production. *Science* 281 (5374), 200–206.

- Faust, B.C., Zepp, R.G., 1993. Photochemistry of aqueous iron(III)-polycarboxylate complexes: roles in the chemistry of atmospheric and surface waters. *Environmental Science & Technology* 27 (12), 2517–2522.
- Fehsenfeld, F., et al., 1992. Emissions of volatile organic compounds from vegetation and the implications for atmospheric chemistry. *Global Biogeochemical Cycles* 6 (4), 389–430.
- Fung, I.Y., et al., 2000. Iron supply and demand in the upper ocean. *Global Biogeochemical Cycles* 14, 281–296.
- Gao, Y., Arimoto, R., Zhou, M.Y., Lee, D.S., Duce, R.A., 1992. Input of atmospheric trace elements and mineral matter to the Yellow Sea during the spring of low dust year. *Journal of Geophysical Research-Atmosphere* 97 (4), 3677–3777.
- Gao, Y., et al., 1997. Temporal and spatial distribution of dust and its deposition to the China Sea. *Tellus B* 49 (2), 172–189.
- Gao, Y., Anderson, J.R., Hua, X., 2007. Dust characteristics over the North Pacific observed through shipboard measurements during the ACE-Asia Experiment. *Atmospheric Environment* 41 (36), 7907–7922.
- Graber, E.R., Rudich, Y., 2006. Atmospheric HULIS: how humic-like are they? A comprehensive and critical review. *Atmospheric Chemistry and Physics* 6, 729–753.
- Guieu, C., et al., 1997. Atmospheric input of dissolved and particulate metals to the northwestern Mediterranean. *Deep-Sea Research II* 44, 655–674.
- Hand, J.L., et al., 2004. Estimates of atmospheric-processed soluble iron from observations and a global mineral aerosol model: biogeochemical implications. *Journal of Geophysical Research* 109, D17205.
- Harrison, R.M., Pio, C.A., 1983. Size-differentiated composition of inorganic atmospheric aerosols of both marine and polluted continental origin. *Atmospheric Environment* 17 (9), 1733–1738.
- He, K.B., et al., 2001. The characteristics of PM_{2.5} in Beijing, China. *Atmospheric Environment* 35, 4950–4970.
- Herner, J.D., et al., 2006. Dominant mechanisms that shape the airborne particle size and composition in central California. *Aerosol Science and Technology* 40, 827–844.
- Hlavay, J., Polyak, K., Molnar, A., Meszaros, E., 1998. Determination of the distribution of elements as a function of particle size in aerosol samples by sequential leaching. *Analyst* 123, 859–863.
- Hoffmann, P., et al., 1996. Speciation of iron in atmospheric aerosol samples. *Journal of Aerosol Science* 27, 325–337.
- Hopper, J.F., Barrie, L.A., 1988. Regional and background aerosol trace elemental composition observed in eastern Canada. *Tellus* 40B, 446–462.
- Horvath, H., Kasahara, M., Pesava, P., 1996. The size distribution and composition of the atmospheric aerosol at a rural and nearby urban location. *Journal of Aerosol Science* 27 (3), 417–435.
- Hutchins, D.A., Bruland, K.A., 1998. Iron-limited diatom growth and Si:N ratios in a coastal upwelling region. *Nature* 393, 561–564.
- Iijima, A., et al., 2008. Emission factor for antimony in brake abrasion dusts as one of the major atmospheric antimony sources. *Environmental Science & Technology* 42, 2937–2942.
- Infante, R., Acosta, I.L., 1991. Size distribution of trace metals in Ponce, Puerto Rico air particulate matter. *Atmospheric Environment* 25B, 121–131.
- Jickells, T.D., 1998. Nutrient biogeochemistry of the coastal zone. *Science* 281 (5374), 217–222.
- Jickells, T.D., Spokes, L.J., 2001. Atmospheric Iron Inputs to the Ocean, in *Biogeochemistry of Iron in Seawater*. John Wiley, Hoboken NJ.
- Johansen, A.M., Siefert, R.L., Hoffmann, M.R., 2000. Chemical composition of aerosols collected over the tropical North Atlantic Ocean. *Journal of Geophysical Research* 105, 15,277–15,312.
- John, W., Wall, S.M., Ondo, J.L., Winklmavr, W., 1990. Models in the size distributions of atmospheric inorganic aerosol. *Atmospheric Environment* 24A, 2349–2359.
- Johnson, K.S., 2001. Iron supply and demand in the upper ocean: is extraterrestrial dust a significant source of bioavailable iron? *Global Biogeochemical Cycles* 15 (1), 61–63.
- Journet, E., Desboeufs, K.V., Caquineau, S., Colin, J.L., 2008. Mineralogy as a critical factor of dust iron solubility. *Geophysical Research Letters* 35, L07805.
- Juichang, R., Freedman, B., Coles, C., Zwicker, B., Holzbecker, J., Chatt, A., 1995. Vanadium contamination of lichens and tree foliage in the vicinity of three oil-fired power plants in eastern Canada. *Journal of the Air & Waste Management Association* 45 (6), 461–464.
- Kane, M.M., Rendell, A.R., Jickells, T.D., 1994. Atmospheric scavenging processes over the North Sea. *Atmospheric Environment* 28, 2523–2530.
- Kaneyasu, K., Yoshikado, H., Mizuno, T., Sakamoto, K., Soufuku, M., 1999. Chemical forms and sources of extremely high nitrate and chloride in winter aerosol pollution in Kanto plain of Japan. *Atmospheric Environment* 33, 1745–1756.
- Kawamura, K., Kaplan, I.R., 1987. Motor exhaust emissions as a primary source for dicarboxylic acids in Los Angeles ambient air. *Environmental Science & Technology* 27, 105–110.
- Kawamura, K., Ng, L.L., Kaplan, L.R., 1985. Determination of organic acids (C1–C10) in the atmosphere, motor exhausts, and engine oils. *Environmental Science & Technology* 19 (11), 1082–1086.
- Kawamura, K., Kasukabe, H., Yasai, O., Barrie, L., 1995. Production of dicarboxylic acids in the arctic atmosphere at polar sunrise. *Geophysical Research Letters* 22, 1253–1256.
- Kawamura, K., Kasukabe, H., Barrie, L., 1996. Source and reaction pathways of dicarboxylic acids, ketoacids and dicarboxylic acids in Arctic aerosols: one year of observations. *Atmospheric Environment* 30, 1709–1722.
- Kawamura, K., Narukawa, M., Li, S.M., Barrie, L., 2007. Size distributions of dicarboxylic acids and inorganic ions in atmospheric aerosols collected during polar sunrise in the Canadian high Arctic. *Journal of Geophysical Research* 112, D10307.
- Kaye, G.W.C., Laby, T.H., 1986. Tables of physical and chemical constants. Longman, NY.
- Keene, W.C., Galloway, J.N., 1986. Considerations regarding sources of formic and acetic acids in the troposphere. *Journal of Geophysical Research* 91, 14466–14474.
- Kerminen, V.M., Wexler, A.S., 1995. Growth laws for atmospheric aerosol particles: an examination of the bimodality of the accumulation mode. *Atmospheric Environment* 29, 3263–3275.
- Khwajia, H.A., 1995. Atmospheric concentrations of carboxylic acids and related compounds at a semiurban site. *Atmospheric Environment* 29, 127–139.
- Kieber, R.J., Skrabal, S.A., Smith, B.J., Willey, J.D., 2005. Organic complexation of Fe(II) and its impact on the redox cycling iron in rain. *Environmental Science & Technology* 39, 1576–1583.
- Kleeman, M.J., Schauer, J.J., Cass, G.R., 2000. Size and composition distribution of fine particulate matter emitted from motor vehicles. *Environmental Science & Technology* 34 (7), 1132–1142.
- Leck, C., Rodhe, H., 1991. Emissions of marine biogenic sulfur to the atmosphere of northern Europe. *Journal of Atmospheric Chemistry* 12, 63–86.
- Li-Jones, X., Prospero, J.M., 1998. Variations in the size distribution of non-sea-salt sulfate aerosol in the marine boundary layer at Barbados: impact of African dust. *Journal of Geophysical Research* 103 (D13), 16073–16084.
- Lin, J.J., 2002. Characterization of water-soluble ion species in urban ambient particles. *Environment International* 28, 55–61.
- Luo, C., Mahowald, N., Bond, T., Chuang, P.Y., Artaxo, P., Siefert, R., Chen, Y., Schauer, J., 2008. Combustion iron distribution and deposition. *Global Biogeochemical Cycles* 22, GB1012.
- Lyons, J.M., Venkataraman, C., Main, H.H., Friedlander, S.K., 1993. Size distribution of trace metals in the Los Angeles atmosphere. *Atmospheric Environment* 27b, 237–249.
- Majestic, B.J., et al., 2006. Development of a wet-chemical method for the speciation of iron in atmospheric aerosols. *Environmental Science & Technology* 40, 2346–2351.
- Malm, W.C., Sisler, J.F., 2000. Spatial patterns of major aerosol species and selected heavy metals in the United States. *Fuel Processing Technology* 65–66, 473–501.
- Martin, J.H., 1990. Glacial–interglacial CO₂ change: the iron hypothesis. *Paleoceanography* 5, 1–13.
- McTainsh, G.H., Walker, P.H., 1982. Nature and distribution of Harmattan dust. *Zeitschrift fuer Geomorphologie* 26, 417–435.
- Meng, Z.Y., Seinfeld, J.H., 1994. On the source of the submicrometer droplet mode of urban and regional aerosols. *Aerosol Science and Technology* 20 (3), 253–265.
- Millero, F.J., Sohn, M.L., 1992. *Chemical Oceanography*. CRC Press, Boca Raton, Fla.
- Mochida, M., et al., 2003. Spatial distributions of oxygenated organic compounds (dicarboxylic acids, fatty acids, and levoglucosan) in marine aerosols over the western Pacific and off the coast of East Asia: continental outflow of organic aerosols during the ACE-Asia campaign. *Journal of Geophysical Research* 108 (D23), 8638.
- Morel, F.M.M., Price, N.M., 2003. The biogeochemical cycles of trace metals in the oceans. *Science* 300 (5621), 944–947.
- Mucha, A.P., Almeida, C.M.R., Bordalo, A.A., Vasconcelo, M.T.S.D., 2005. Exudation of organic acids by a marsh plant and implications on trace metal availability in the rhizosphere of estuarine sediments. *Estuarine, Coastal and Shelf Science* 65, 191–198.
- Novakov, T., Hegg, D.A., Hobbs, P.V., 1997. Airborne measurements of carbonaceous aerosols on the East Coast of the United States. *Journal of Geophysical Research* 102 (D25), 30,023–30,030.
- Nriagu, J.O., 1989. A global assessment of natural sources of atmospheric trace metals. *Nature* 338, 47–49.
- Nriagu, J.O., Pacyna, J.M., 1988. Quantitative assessment of worldwide contamination of air, water and soils by trace metals. *Nature* 333, 134–139.
- Ooki, A., Nishioka, J., Ono, T., Noriki, S., 2009. Size dependence of iron solubility of Asian mineral dust particles. *Journal of Geophysical Research* 114, D03202.
- Pakkanen, T.A., 1996. Study of formation of coarse particles nitrate aerosol. *Atmospheric Environment* 30 (14), 2475–2482.
- Pakkanen, T.A., et al., 2001. Sources and chemical composition of atmospheric fine and coarse particles in the Helsinki area. *Atmospheric Environment* 35, 5381–5391.
- Pathak, R.K., Yao, X.H., Chan, C.K., 2004. Sampling artifacts of acidity and ionic species in PM_{2.5}. *Environmental Science & Technology* 38 (1), 254–259.
- Pehkonen, S.O., Siefert, R., Erel, Y., Webb, S., Hoffmann, M.R., 1993. Photoreduction of iron oxyhydroxides in the presence of important atmospheric organic compounds. *Environmental Science & Technology* 27, 2056–2062.
- Pike, S.M., Moran, S.B., 2001. Trace elements in aerosol and precipitation at New Castle, NH, USA. *Atmospheric Environment* 35 (19), 3361–3366.
- Sannigrahi, P., Sullivan, A.P., Weber, R.J., Ingall, E.D., 2005. Characterization of water-soluble organic carbon in urban atmospheric aerosol using solid-state ¹³C NMR spectroscopy. *Environmental Science & Technology* 40, 666–672.
- Savoie, D.L., Prospero, J.M., 1982. Particle size distribution of nitrate and sulphate in the marine atmosphere. *Geophysical Research Letter* 9, 1207–1210.
- Saydam, A.C., Senyuva, H.Z., 2002. Desert: can they be the potential suppliers of bioavailable iron? *Geophysical Research Letters* 29 (11), 1524.
- Schaap, M., Spindler, G., Schulz, A., Maenhaut, W., Berner, A., 2004. Artifacts in the sampling of nitrate studied in the “INTERCOMP” campaigns of EUROTRAC-AEROSOL. *Atmospheric Environment* 38, 6487–6496.
- Sedlak, D.L., Hoigné, J., 1993. The role of copper and oxalate in the redox cycling of iron in atmospheric waters. *Atmospheric Environment* 27A, 2173–2185.
- Sedwick, P.N., Sholkovitz, E.R., Church, T.M., 2007. Impact of anthropogenic combustion emissions on the fractional solubility of aerosol iron: evidence from the Sargasso Sea. *Geochemistry Geophysics Geosystems* 8, 1–21.
- Sholkovitz, E.R., Sedwick, P.N., Church, T.M., 2009. Influence of anthropogenic combustion emissions on the deposition of soluble aerosol iron to the ocean: empirical estimates for island sites in the North Atlantic. *Geochimica et Cosmochimica Acta* 73, 3981–4003.
- Siefert, R.L., Pehkonen, S.O., Erel, Y., Hoffman, M.R., 1994. Iron photochemistry of aqueous suspensions of ambient aerosol with added organic acids. *Geochimica et Cosmochimica Acta* 58, 3271–3279.
- Siefert, R.L., Johansen, A.M., Hoffmann, M.R., 1999. Chemical characterization of ambient aerosol collected during the southwest monsoon and intermonsoon seasons over the Arabian sea: labile-Fe(II) and other trace metals. *Journal of Geophysical Research* 104, 3511–3526.

- Song, X.-H., Polissar, A.V., Hopke, P.K., 2001. Sources of fine particle composition in the northeastern US. *Atmospheric Environment* 35 (31), 5277–5286.
- Spokes, L.J., Jickells, T.D., 1996. Factors controlling the solubility of aerosol trace metals in the atmosphere and on mixing into seawater. *Aquatic Geochemistry* 1, 355–374.
- Spokes, L.J., Jickells, T.D., Lim, B., 1994. Solubilisation of aerosol trace metal by cloud processing: a laboratory study. *Geochimica et Cosmochimica Acta* 58 (15), 3281–3287.
- Spurny, K.R., 2000. *Aerosol chemical processes in the environment*. Lewis Publisher, Boca Raton, FL.
- Stookey, L.L., 1970. Ferrozine – a new spectrophotometric reagent for iron. *Analytical Chemistry* 42 (7), 779–781.
- Sunda, W.G., 2001. *The biogeochemistry of iron in seawater: 3. Bioavailability and bioaccumulation of iron in the sea*. John Wiley, Hoboken NJ.
- Talbot, R.W., Beecher, K.M., Harris, R.C., Cofer, W.R., 1988. Atmospheric geochemistry of formic and acetic acids at a midlatitude temperate site. *Journal of Geophysical Research* 93, 1638–1652.
- Taylor, S.R., McLennan, S.M., 1985. *The continental crust: its composition and evolution*. Blackwell, Oxford.
- Tolocka, M.P., et al., 2001. East versus west in the US: chemical characteristics of PM_{2.5} during the winter of 1999. *Aerosol Science and Technology* 34, 88–96.
- Visser, F., Gerringa, L.J.A., Gaast, S.J.V.D., Baar, H.J.W.D., Timmermans, K.R., 2003. The role of the reactivity and content of iron of aerosol dust on growth rates of two Antarctic diatom species. *Journal of Phycology* 29, 1085–1094.
- Warneck, P., 2003. In-cloud chemistry opens pathways to the formation of oxalic acid in the marine atmosphere. *Atmospheric Environment* 37, 2423–2427.
- Whelpdale, D.M., Moody, J.L., 1990. Large-scale meteorological regimes and transport processes. In: Knap, A.H. (Ed.), *The long range transport of natural and contaminant substances*. Kluwer, Dordrecht.
- Wu, P.M., Okada, K., 1994. Nature of coarse nitrate particles in the atmosphere – a single particle approach. *Atmospheric Environment* 28, 2053–2060.
- Xu, N., Gao, Y., 2008. Characterization of hematite dissolution affected by oxalate coating, kinetics and pH. *Applied Geochemistry* 23 (4), 783–793.
- Yaqub, R.R., Davies, T.D., Jickells, T.D., Miller, J.M., 1991. Trace elements in daily collected aerosols at a site in southeast England. *Atmospheric Environment* 25, 985–996.
- Zhao, Y., Gao, Y., 2008. Mass size distributions of water-soluble inorganic and organic ions in size-segregated aerosols over metropolitan Newark in the US East Coast. *Atmospheric Environment* 42 (18), 4063–4078.
- Zhu, X., Prospero, J.M., Millero, F.J., Savoie, D.L., Brass, G.W., 1992. The solubility of ferric iron in marine aerosol solutions at ambient relative humidity. *Marine Chemistry* 38, 91–107.
- Zhu, X., Prospero, J.M., Millero, F.J., 1997. Diel variability of soluble Fe(II) and soluble total Fe in North African dust in the trade winds at Barbados. *Journal of Geophysical Research* 102, 21,297–21,305.
- Zhuang, G., Yi, Z., Duce, R.A., Brown, P.R., 1992a. Link between iron and sulphur cycles suggested by detection of Fe(n) in remote marine aerosols. *Nature* 355, 537–539.
- Zhuang, G., Yi, Z., Duce, R.A., Brown, P.R., 1992b. Chemistry of iron in marine aerosols. *Global Biogeochemical cycles* 6 (2), 161–173.
- Zhuang, H., Chan, C.K., Fang, M., Wexler, A.S., 1999. Size distributions of particulate sulfate, nitrate, and ammonium at a coastal site in Hong Kong. *Atmospheric Environment* 33 (6), 843–853.
- Zoller, W.H., Gladney, E.S., Duce, R.A., 1974. Atmospheric concentrations and sources of trace metals at the South Pole. *Science* 183, 198–200.
- Zuo, Y., 1995. Kinetics of photochemical/chemical cycling of iron coupled with organic substances in cloud and fog droplets. *Geochimica et Cosmochimica Acta* 59, 3123–3131.
- Zuo, Y., Hoigné, J., 1992. Formation of hydrogen-peroxide and depletion of oxalic-acid in atmospheric water by photolysis of iron(III)-oxalate complexes. *Environmental Science & Technology* 26 (5), 1014–1022.